ELSEVIER

Palaeogeography, Palaeoclimatology, Palaeoecology 131 (1997) 391–412

PALAEO

The late Quaternary calcareous nannoplankton assemblages from three cores from the Tasman Sea

Chikara Hiramatsu *, Patrick De Deckker

Department of Geology (The Australian Marine Quaternary Program), The Australian National University, Canberra, ACT 0200, Australia

Received 11 May 1995; accepted 15 January 1996

Abstract

The composition of the late Quaternary calcareous nannoplankton in three deep-sea cores RC12-113, Z-2108 and GC-3, located along a N–S transect at three different latitudes (25°, 33°, 44°S) in the Tasman Sea, has been investigated. The shift in floral dominance from small *Gephyrocapsa* to small placoliths (labelled here "Small Placolith"), and then to *Emiliania huxleyi* is recognized at stage 5 and stage 4, respectively, in cores RC12-113 and Z-2108. However, the occurrence of small *Gephyrocapsa* and Small Placolith displays a seesaw relationship in core GC-3 which is located today just north of the Subtropical Convergence, east of Tasmania. *Gephyrocapsa muellerae* and *Coccolithus pelagicus* increase their abundance geographically southwards and stratigraphically during glacial periods, whereas the percentage abundances of *Florisphaera profunda* and *Umbilicosphaera sibogae* demonstrate reverse patterns. The relationships between the percentage abundance of each nannoplankton species and the $\delta^{18}O$ record for three cores are discussed in detail.

A transfer function for estimating past sea-surface temperatures (=TN) is attempted here; it is based on core-top data from the Tasman Sea and provides a good relationship between some calcareous nannoplankton assemblages and modern mean summer sea-surface temperatures. The TN value shows a good correspondence with the $\delta^{18}O$ record in all three cores.

Core GC-3 is much affected by $CaCO_3$ dissolution in comparison with cores RC12-113 and Z-2108. The calcareous nannoplankton dissolution patterns recognized in the three cores do not show a systematic correspondence with the $\delta^{18}O$ record. Of interest, however, is the good preservation peaks that are recognized in all three cores at the transitions from glacial to interglacial events. © 1997 Elsevier Science B.V.

Keywords: calcareous nannoplankton; palaeoceanography; Tasman Sea

1. Introduction

There are few studies on the late Quaternary palaeoceanography of the oceans surrounding Australia that are based on calcareous nannoplankton. Of importance is the work of Okada and Wells (1994) who investigated several cores from offshore Western Australia. Several other studies, nevertheless, have resulted from the DSDP Leg 90 on the Lord Howe Rise. These are the work of Lohman (1986) who reconstructed a Neogene and Quaternary biostratigraphy for the southern Coral Sea, Tasman Sea and southwestern

* Corresponding author. Present address: JAPEX Research Center, 1-2-1 Hamada, Mihama-ku, Chiba, 261 Japan.

PII S0031-0182(97)00013-8

Pacific Ocean. The works of Nelson et al. (1985), and Dudley and Nelson (1988, 1989) followed on by presenting the first stable-isotopic studies of calcareous nannoplankton for the region, with emphasis paid on the $\delta^{13}C$ signatures in these nannofossils as an indicator of palaeoproductivity for the region. The present study provides new data on late Quaternary calcareous nannoplankton from 3 cores located along a N–S transect in the southern Coral and Tasman Seas.

This project benefited from a recent study of the distribution of calcareous nannoplankton in surface sediment in the Tasman and Coral Seas (Hiramatsu and De Deckker, 1997-this issue). For that study, sediment recovered from inside foraminifera tests was examined from 53 core-top samples widely spaced in the above-mentioned two seas. The relationship between the percentage abundance of each nannoplankton species and summer sea-surface temperature (SST), and the relationship between species composition and the position of oceanic fronts were discussed in detail (Hiramatsu and De Deckker, 1997-this issue). Nevertheless, encouraging results indicated that floral composition is considerably controlled by SST, suggesting the possibility of using calcareous nannoplankton for estimating of past SST for the Western Pacific.

In the present paper, data from Hiramatsu and De Deckker's (1997-this issue) 53 core tops are applied to the late Quaternary assemblages recovered from three cores studied here. Calcareous nannoplankton assemblages were sampled in detail in all three cores with the aim to reconstruct the palaeoceanographic history of the Tasman Sea, and to build up a stratigraphic framework for the late Quaternary of the region. Moreover, the relationship between the percentage abundance of each species in 3 cores and the $\delta^{18}O$ record is also investigated in an attempt to decipher any possible signals of climatic change through the intermediary of calcareous nannoplankton.

2. Materials and methods

Three cores, taken from the Tasman Sea, were used for this study. From north to south, these are: core RC12-113 (lat. 24°53′S, long. 163°31′E, 2454-m water depth) from the northern portion of the Lord Howe Rise; core Z-2108 (lat. 33°23′S, long. 161°37′E, 1448-m water depth) from the southern portion of the Lord Howe Rise; and core GC-3 (lat. 44°15′S, long. 149°59′E, at 2667-m water depth) was collected on the East Tasman Plateau (Fig. 1). These cores are located near the present position of the southern Tropical Convergence, the Tasman Front and the Subtropical Convergence, respectively (Fig. 1). Samples were examined at 10-cm intervals for the upper 2 m of core RC12-113 and the entire of core Z-2108 which is 4 m long, and at 5-cm intervals for core GC-3 which is 4.7 m long.

Smear slides were prepared for microscopic observation by using unprocessed sediment samples from cores RC12-113 and GC-3. Smear slides were made from sediment preserved inside the globular foraminifera *Orbulina universa* recovered from core Z-2108. The similarity in floral compositions between the inside of a foraminifer and its surrounding matrix sediment was discussed in Hiramatsu and De Deckker (1997-this issue).

A stepwise counting method (Okada, 1992) was used throughout the study. More than 500 specimens first encountered for each sample were identified (=Step 1). After the first counting, major species such as *Emiliania huxleyi*, *Florisphaera profunda*, all species grouped under the genus *Gephyrocapsa* and Small Placolith (<2.5 μm) [see taxonomic notes below] were eliminated from counting during the next procedure (=Step 2). More than 300 specimens, exclusive of those dominant taxa, were identified in the second counting. This provided a comprehensive list of the subdominant taxa. All samples were observed under a polarising microscope at 1600× magnification.

3. Taxonomic notes

E. huxleyi is a complex species characterized by several morphotypes. Genotypic variation of this species was studied in detail by Young and Westbroek (1991) on the basis of a biometric examination of numerous specimens. The recent, local study of Hiramatsu and De Deckker (1996)

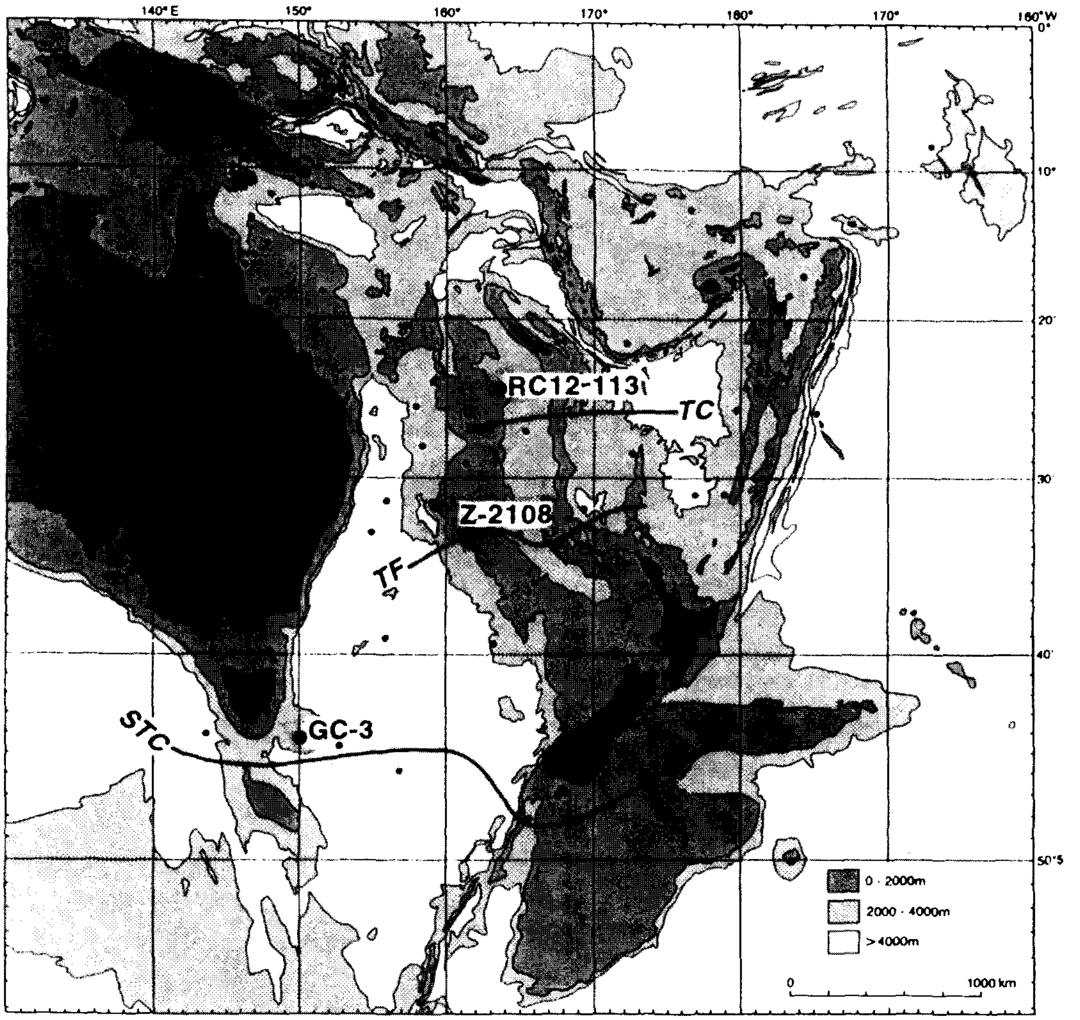

Fig. 1. Locality map of cores RC12-113, Z-2108 and GC-3. The position of the Tropical Convergence (*TC*), the Tasman Front (*TF*) and the Subtropical Convergence (*STC*) are also identified.

of living coccolithophorids sampled near the Subtropical Convergence southeast of Tasmania suggests that at least two morphotypes of this taxon can be recognized in the area. These authors established a good correlation between each morphotype and sea-surface temperature, although it is likely that the extent of calcification for two morphotypes is related to calcite saturation at the sea surface, and thus p_{CO_2} and temperature being interrelated with the former. Unfortunately, it is impossible to precisely identify morphological differences in this small species under a polarising microscope. Hence, the different morphotypes of *E. huxleyi* were not considered in the present study.

F. profunda, first described from the Pacific Ocean by Okada and Honjo (1973), is divided into two varieties, *F. profunda* var. *profunda* and *F. profunda* var. *elongata* (Okada and McIntyre, 1977). Both varieties were observed in the cores, but the latter variety was poorly represented in this study. As a consequence, both varieties were lumped together simply as *F. profunda*.

The name of *Gephyrocapsa* sp. (closed) was given for a specimen belonging to *Gephyrocapsa* with a closed central area. This phenomenon was similar for *Reticulofenestra perplexa/productus* when examined under the microscope. These taxa apparently have a convex central area, similar in structure to the distal shield of genus *Gephyrocapsa* when examined under SEM view (Plate I, A–C). *Gephyrocapsa* sp. (closed) is considered to belong to *G. caribbeanica* which is heavily calcified and filled in central opening, because of the existence of transition form to both types and with similar stratigraphic occurrences in core GC-3.

The term "small *Gephyrocapsa*" was used for *Gephyrocapsa* specimens smaller than 2.5 μm in overall coccolith size (Plate I, D and E). Small *Gephyrocapsa* specimens principally belong to *G. aperta* and *G. ericsonii*.

"Small Placolith" was termed for placoliths smaller than 2.5 μm and without a central bridge. These specimens are thought to represent either "small *Gephyrocapsa*" species but which do not have central bridge, or small *Reticulofenestra* species (Plate I, F–H).

4. Calcareous nannoplankton assemblages from deep-sea cores from the Tasman Sea

4.1. Core RC12-113 (Table 1)

The isotope stratigraphy of this core, based on the $\delta^{18}O$ of *Globigerinoides sacculifer*, was taken from the work of Anderson et al. (1989) and the composition of planktonic foraminiferal assemblages from Martinez (1994). An $AMS^{14}C$ date of 13,395 yr BP was determined for a sample taken at a depth of 25 cm in this core. The last glacial maximum (LGM) is recognized at a depth of 40 cm in this core (Anderson et al., 1989).

Figs. 2a and b displays the stratigraphic occurrence of major species encountered in this core. *Emiliania huxleyi* increases in dominance up-core, and is particularly dominant during stages 4–2. This species again decreases at stage 1 in contrast to *F. profunda*. The horizon characterized by dominant occurrence of *E. huxleyi* (0–70 cm) is correlated to Gartner's *E. huxleyi* acme zone which spans the last 70 kyr BP (Gartner, 1977), whereas it spans the last 85 kyr BP in tropical and subtropical waters and the last 73 kyr BP in transitional waters (Thierstein et al., 1977). *E. huxleyi* shows a small abundance increase during stage 6. "Small Placolith" is abundant through stages 7 to 5, and decreases in abundance during stages 4–2. It seems that *E. huxleyi* is the taxon that replaces "Small Placolith", thus perhaps taking its ecological niche. Small *Gephyrocapsa* is abundant during stage 7, but then decreases progressively towards the top of the core. Small *Gephyrocapsa* is very rare in levels younger than stage 5. *F. profunda* is dominant during the Holocene, and relatively abundant during interglacial periods, whereas the percentage abundance of this species decreases during glacial periods. This stratigraphic change in abundance of *F. profunda* is predicted from its geographic distribution of surface sediment samples (Hiramatsu and De Deckker, 1997-this issue) which identifies that this species is dominant in low latitudes and rare in high latitudes. *G. muellerae*, which is a high-latitude species in the Tasman Sea, increases its abundance during stages 6 and 4–2. *G. oceanica* does not show a systematic correspondence with the $\delta^{18}O$ record, but appears to increase in number below the 100-cm level. *Gephyrocapsa* sp. (closed) and *G. caribbeanica* occur throughout the core, but in low number.

Among the subdominant species, middle to low latitudes species such as *Neosphaera coccolithomorpha*, *Oolithotus fragilis*, *Rhabdosphaera clavigera* and *Umbilicosphaera sibogae* are abundant in this core because it benefits from being in the most northern location of the three cores studied. Not surprisingly, *Coccolithus pelagicus*, which is abundant south of the Subtropical Convergence based on the study of Hiramatsu and De Deckker (1997-this issue), is extremely rare in core RC12-113.

The percentage abundance of *Acanthoica* spp. increases during stage 5 and decreases for stages 6 and 4–2. *Calcidiscus leptoporus* is the major species among the subdominant species in this core, but less so in comparison with the other two cores; it is characteristically a high-latitude species as documented through the study of modern samples of Hiramatsu and De Deckker (1997-this issue). The percentage abundance of *C. leptoporus* is high during stages 7 and 6, but shows significant reduc-

Table 1
Species occurrence chart for all species recovered in core RC12-113

RC12-113	Sample Depth (cm)	2-3	9-10	19-20	30-31	40-41	51.5-52.5	59-60	69-70	80-81	89-90	99-100	109-110	119-120	129-130	139-140	149-150	160-161	169-170	179-180	189-190	199-200
Abundance		A	A	A	A	A	A	A	A	A	A	A	A	A	A	A	A	A	A	A	A	A
Preservation	perfect C. lept.%	59	61	78	68	63	62	64	61	56	57	61	60	65	64	58	53	48	57	33	50	49
Step 1																						
Emiliania	huxleyi	112	103	257	216	240	256	242	214	123	119	84	56	58	99	73	61	47	16	8	17	22
Florisphaera	profunda	351	370	175	172	108	121	126	153	183	185	193	230	221	161	167	132	254	194	172	202	104
Gephyrocapsa	aperta				1	2	4	4	2	2	8	12	71	50	37	75	71	68	181	169	141	111
Gephyrocapsa	caribbeanica			1				1	2	1		1			4	1		3	3	5	6	31
Gephyrocapsa	ericsonii											4	3	1	3	1		4	7	7	8	2
Gephyrocapsa	muellerae	4	4	11	31	18	38	28	37	25	18	12	12	17	24	26	34	10	4	14	10	37
Gephyrocapsa	oceanica	3	7	10	22	12	13	26	13	13	21	18	12	31	33	24	35	37	20	36	32	48
Gephyrocapsa	sp.(closed)	2	1	4	3	2	6	1	7	2	5	3	5	1	5	3	3	5	4	6	8	45
Small Placolith	(< 2.5um)	2	4	4	9	16	42	42	30	95	73	107	91	75	75	62	40	46	83	47	70	94
Subdominant taxa		31	24	49	66	103	53	52	78	57	78	72	31	65	60	94	132	31	29	36	49	39
	Total	505	513	511	520	501	533	522	536	501	507	506	511	519	501	526	508	505	541	500	543	533
Step 2																						
Acanthoica	spp.		5	2	5		1	4	2	3	5	8	2	4		2	3	1	4		3	3
Calcidiscus	leptoporus	51	47	41	42	54	51	55	69	35	55	40	37	78	70	87	72	52	95	93	102	112
Calciosolenia	murrayi	37	32	18	28	15	30	15	14	22	12	19	32	11	21	12	11	27	31	23	18	20
Ceratolithus	spp.		1			3																
Coccolithus	pelagicus			1							1							1				
Discosphaera	tubifera				1																	
Helicosphaera	carteri	1	14	11	8	11	6	12	18	7	13	6	9	12	23	44	38	14	7	16	25	25
Helicosphaera	pavimentum		1	1			1	1	1					1		1				1		
Neosphaera	coccolithomorpha	84	63	57	66	45	46	58	57	55	47	58	56	52	53	35	47	50	63	49	47	33
Oolithotus	fragilis	45	32	46	47	85	72	69	44	66	66	61	59	72	51	46	54	42	31	35	57	55
Pontosphaera	japonica	1	2	2		1		1	1		1			1		2						
Pontosphaera	multipora																1	1			1	2
Rhabdosphaera	clavigera	14	25	20	26	21	31	20	30	45	38	17	24	18	28	22	29	43	19	24	20	20
Syracosphaera	spp.	13	30	39	27	27	28	36	25	25	20	18	32	15	30	25	27	21	17	19	15	13
Tetralithoides	quadrilaminata					1	1					1	3		2	1		1		1		
Thoracosphaera	spp.					2								1							1	
Umbellosphaera	irregularis	6	6	10	8	3	3	5	1	10	5	9	17	7	2	3	13	19	1	2	1	4
Umbellosphaera	tenuis	18	24	33	25	15	9	14	14	8	12	9	2	2	1		3	2	4	10	1	3
Umbilicosphaera	hulburtiana	1	1	1	1		1					1	2		1			3	1	2		
Umbilicosphaera	sibogae	32	31	20	19	23	23	20	27	24	27	55	30	27	22	22	11	26	27	29	18	19
Subdominant taxa	Total	303	314	302	303	306	303	310	303	300	302	302	305	301	304	302	309	303	300	304	309	309
	Reworked specimens	0	0	0	0	0	0	0	0	1	0	0	1	0	0	1	0	1	0	0	0	0

tion for stage 5. The abundance of this species with respect to other taxa does not show an obvious change between stages 2 and 1. The occurrence of *Calciosolenia murrayi* is characterized by many high-amplitude, short-term fluctuations throughout the core. However, there is no obvious relationship between this species and the $\delta^{18}O$ record. The percentage abundance of *Helicosphaera carteri* displays a prominent peak at stage 6, but with no significant change afterwards for stages 5–1. *N. coccolithomorpha* seems to decrease in abundance slightly during glacial intervals, whereas *O. fragilis* retains a high abundance through stages 6–2. The abundance of *R. clavigera* maintains values between 5% and 10%, except for two peaks at the late stage 7 and the late stage 5. *Syracosphaera* spp. also maintain their abundance between 5% and 10% throughout this core, but there is no significant relationship with the $\delta^{18}O$ record. *Umbellosphaera irregularis* increases in abundance during interglacial periods and has substantially lower values during stages 6 and 4–2. The percentage abundance of *Umbellosphaera tenuis* shows a conspicuous reduction during stage 6, and shows a downward trend afterwards. This species is common during the Holocene, but values are not as high as for stage 5. The percentage abundance of *Umbilicosphaera sibogae* is somewhat lower during the glacial periods.

PLATE I

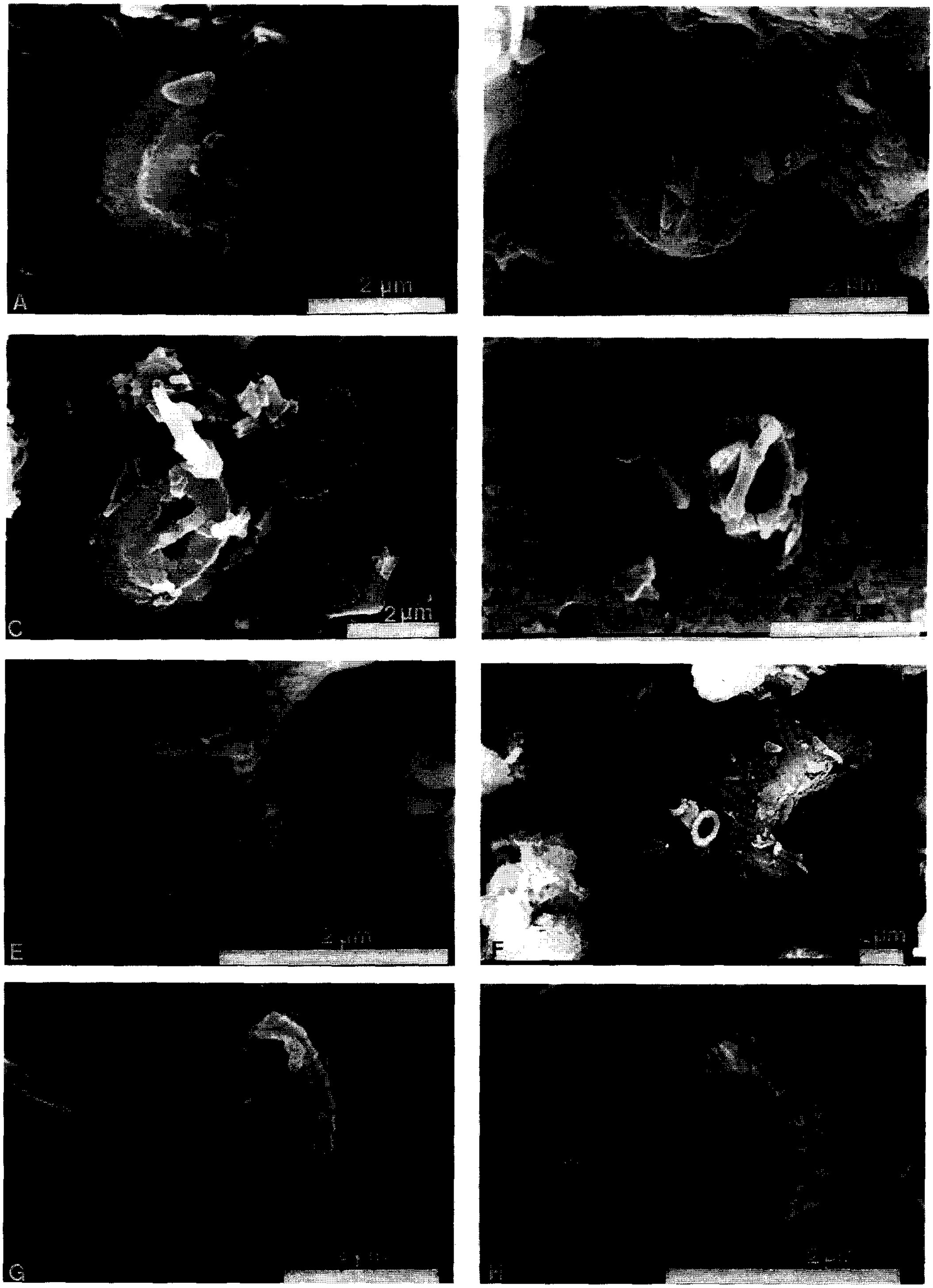

4.2. Core Z-2108 (Table 2)

Core Z-2108 is located today near the Tasman Front. The $\delta^{18}O$ and $\delta^{13}C$ of *Globigerina bulloides* and *Uvigerina* spp., measured by Nelson et al. (1993), are used here to establish a chronology for this core. The aeolian quartz content of core Z-2108 was also studied by Thiede (1979).

E. huxleyi shows an upward trend of increasing abundance, and predominates all other taxa for stages 4 to 1. This pattern is similar in core RC12-113 (Fig. 2a) and can thus be used as a means for stratigraphic correlation. Small Placolith is abundant during stages 7 to 4, and with particularly high values for the middle of stage 5 and the stage 4 transition. Small Placolith is rare in the younger levels. The shift in floral dominance from small *Gephyrocapsa* to Small Placolith, and then to *E. huxleyi* is recognized through the stage 5–4 transition in both cores RC12-113 and Z-2108. This stratigraphic/ecological succession of dominance among the phylogenetically related taxa of *Emiliania huxleyi*, Small Placolith and small *Gephyrocapsa* has already been discussed by Okada and Wells (1994) for offshore Western Australia in two deep-sea cores. These authors emphasized that this shift in floral dominance from small *Gephyrocapsa* — to Small Placolith — to *E. huxleyi* could become a new useful tool for identifying isotope stages 4 and 5. This biostratigraphic indicator is also useful for the middle latitudes in the Tasman Sea. However, as will be seen below, this phenomenon cannot be applied to core GC-3 located further south in the Tasman Sea. It is considered that the southern extent of this biostratigraphic phenomenon using the above-mentioned taxa occurs at the Subtropical Convergence. The percentage abundance of *F. profunda* is high for the Holocene and seems to be low during stage 6. This percentage, ranging from 10% to 30%, is relatively low in comparison with that in core RC12-113 where *F. profunda* ranges from 20% to 40%. This phenomenon is easily explained through the latitudinal distribution of *F. profunda* which is dominant today at low latitudes (Hiramatsu and De Deckker, 1997-this issue). The percentage abundance of *G. muellerae* is apparently higher during glacial periods, and decreases during interglacial periods, although percentage values are apparently high for stage 3. *G. oceanica* is ubiquitous throughout this core, and does not demonstrate a systematic correspondence with the $\delta^{18}O$ record. *Gephyrocapsa* sp. (closed) and *G. caribbeanica* are minor components in this core.

The occurrences of the subdominant taxa from core Z-2108 are described below (see Fig. 3b). The percentage abundance of *Acanthoica* spp. shows many short-term fluctuations, but there are apparently no relationship with the $\delta^{18}O$ record, although it is obvious that the stable-isotope curve is far from matching the standard one of SPECMAP (Martinson et al., 1987). The substantially high peak observed in the middle of stage 5 in core RC12-113 could probably correspond to a similar one in core Z-2108. *C. leptoporus* displays a fluctuating pattern in abundance, but with no obvious relationship with the $\delta^{18}O$ record; this pattern is as expected due to the now-known geographic distribution of this species within surface sediment samples (Hiramatsu and De Deckker, 1997-this issue). The percentage of *C. leptoporus* maintains high values ($\sim$30%) when compared to core RC12-113 since it is more common at higher latitudes today. The percentage abundance of *C. murrayi* also fluctuates throughout this core with no relation to the $\delta^{18}O$ record.

Plate I

Scanning electron microscope photographs:

A. *Gephyrocapsa* sp. (closed) from core RC12-113 at 200-cm depth.
B. *Gephyrocapsa caribbeanica* from core GC-3 at 346-cm depth.
C. *G.* sp (closed) and *G. caribbeanica* from core RC12-113 at 200-cm depth.
D. Small *Gephyrocapsa* from core GC-3 at 235-cm depth.
E. Small *Gephyrocapsa* from core RC12-113 at 120-cm depth.
F. Small Placolith (see *arrow*) on the distal shield of *Coccolithus pelagicus* from core GC-3 at 346-cm depth.
G. Small Placolith from core GC-3 at 346-cm depth.
H. Small Placolith from core RC12-113 at 120-cm depth.

Table 2
Species occurrence chart for all species recovered in core Z-2108

Z-2108 (1/2)	Sample Depth(cm)	5-6	15-16	25-26	35-36	45-46	55-56	65-66	75-76	85-86	95-96	100-101	110-111	120-121	130-131	140-141	150-151	160-161	170-171	180-181	190-191	200-201	205-206	215-216	225-226
Abundance		A	A	A	A	A	A	A	A	A	A	A	A	A	A	A	A	A	A	A	A	A	A	A	A
Preservation	perfect C. lept.%	76	61	61	46	54	58	63	46	59	58	44	60	50	54	60	55	63	52	53	58	58	52	54	66
Step 1																									
Emiliania	huxleyi	227	268	281	184	193	176	151	216	89	154	143	187	216	141	127	65	146	127	91	52	52	37	46	37
Florisphaera	profunda	216	162	103	135	147	134	141	99	63	93	126	119	99	112	106	99	68	85	76	98	87	116	113	94
Gephyrocapsa	aperta	1	2	1	1	6	6	3	2	2	2	3	4	7	13	9	9	22	20	10	53	53	67	100	77
Gephyrocapsa	caribbeanica				4	1	1		2	3	2		1	3		3	1			1	2		2	3	3
Gephyrocapsa	ericsonii					1							1						1	5	7	7	16	10	7
Gephyrocapsa	muellerae	14	18	34	46	43	45	35	55	55	69	89	43	38	44	49	14	9	12	30	9	17	19	21	43
Gephyrocapsa	oceanica	15	16	28	18	17	7	12	19	35	43	18	13	12	12	15	3	17	7	15	14	20	14	20	28
Gephyrocapsa	sp.(closed)		4	4	3	1	1	5	1	3	3	3	1	2	3	2		1	2	3	1		3	3	1
Small Placolith	(< 2.5um)	2	3	4	8	18	13	12	20	4	10	60	62	45	150	178	290	207	231	237	216	236	167	146	74
Subdominant taxa		29	35	68	104	77	119	146	89	249	127	64	71	83	27	27	23	30	16	32	48	49	65	38	144
	Total	504	508	523	503	504	502	505	503	503	503	506	502	505	502	516	504	500	501	500	500	521	506	500	508
Step2																									
Acanthoica	spp.	4	2	1		1	2	1	4				1	1	3	1	2		3	1		1	4	3	3
Calcidiscus	leptoporus	88	83	90	106	107	88	114	82	92	116	98	92	83	66	103	72	92	69	72	116	67	96	82	112
Calciosolenia	murrayi	40	49	28	14	16	28	12	15	1	6	2	19	14	36	6	8	24	26	20	6	29	21	30	5
Ceratolithus	spp.			1							1					1									1
Coccolithus	pelagicus			2	5	7	8	5	3	9		2	8	2	7	7	2	1	1						1
Discosphaera	tubifera					1												1							
Helicosphaera	carteri	13	13	19	36	22	33	40	20	52	45	43	48	26	32	32	22	14	14	26	41	15	27	10	36
Helicosphaera	pavimentum	1		1	6	4	2	1	1		2			1		1	1		1		1	1		2	
Neosphaera	coccolithomorpha	48	46	40	19	25	26	19	31	21	28	20	35	44	34	19	22	25	23	32	17	33	25	40	30
Oolithotus	fragilis	36	34	57	43	52	50	57	71	77	51	55	52	54	42	51	78	59	81	68	47	74	68	69	52
Pontosphaera	japonica				3	1	1	6	1	3		1				1			2	1					1
Pontosphaera	spp.						1			2	1		1												
Rhabdosphaera	clavigera	14	17	6	18	13	13	13	13	15	9	18	14	9	17	19	20	12	13	10	16	11	7	7	8
Syracosphaera	spp.	19	12	17	16	26	21	12	25	11	11	11	17	15	19	9	25	25	13	10	9	16	16	17	6
Tetralithoides	quadrilaminata					1		1								1				2	1		2		
Thoracosphaera	spp.	2			1																				
Umbellosphaera	irregularis	2	3			1	2		3		1	3	3	2	3	2		3	1	2			1	1	
Umbellosphaera	tenuis	8	17	6	6	9	6	2	6	1	3	2	6	11	5	2	1	4	4	1					1
Umbilicosphaera	hulburtiana								2	3		2	2	3	2	1		1		2		3	1	1	1
Umbilicosphaera	sibogae	25	28	34	27	15	19	19	26	13	26	43	29	38	34	46	47	48	53	53	59	51	32	39	44
Subdominant taxa	Total	300	304	302	300	301	300	302	303	300	300	300	327	303	300	302	300	309	304	300	313	301	300	301	301
	Reworked specimens	3	0	2	3	3	0	4	3	1	3	2	2	1	3	0	0	0	3	1	0	2	1	1	0

The percentage shows the highest value during part of the Holocene in cores Z-2108 and RC12-113. The high value at the bottom of core Z-2108 corresponds to a more positive shift in $\delta^{18}O$, which in fact could represent the end of stage 7. *C. pelagicus* apparently increases in abundance during glacial periods, and becomes extremely rare during interglacial periods. According to the investigations done on surface sediment samples (Hiramatsu and De Deckker, 1997-this issue), *C. pelagicus* restrictedly occurs in samples taken south of the Tasman Front. Thus, the occurrence of *C. pelagicus* in core Z-2108 located near the Tasman Front, indicates a more northward movement of the Front during glacial periods. This phenomenon was also recognised by Martinez (1994) for the same area through the investigation of planktonic foraminifera assemblages in several cores. *H. carteri* increases in abundance during stages 6 and 4–2, and decreases during stages 7, 5 and 1. It appears that the percentage abundances of this species show a reverse relationship with the $\delta^{18}O$ record, despite no obvious relationship with SST in the modern surface sediment samples data of Hiramatsu and De Deckker (1997-this issue). A maximum value in abundance for this species during stage 6 follows the trend established in core RC12-113. The percentage abundance of *N. coccolithomorpha* shows a good correspondence with the $\delta^{18}O$ record during stages 7 to late 5, especially with a remarkable reduction at stage 6. The abundance percentage of this species shows relatively low values when compared with core RC12-113. The percentage abundance of *O. fragilis* shows a similar pattern to the $\delta^{18}O$ record. In particular, the substantial decline

Z-2108 (2/2)	Sample Depth(cm)	235-236	245-246	255-256	265-266	275-276	285-286	295-296	305-306	309-310	320-321	330-331	340-341	350-351	360-361	370-371	380-381	390-391	400-401
Abundance		A	A	A	A	A	A	A	A	A	A	A	A	A	A	A	A	A	A
Preservation	perfect C. lept.%	62	71	56	60	57	52	52	65	54	46	52	52	53	46	47	52	45	48
Step 1																			
Emiliania	huxleyi	26	48	74	69	58	69	35	62	71	36	27	51	64	53	57	34	16	14
Florisphaera	profunda	151	120	74	54	47	50	77	69	51	81	68	74	39	74	81	95	105	81
Gephyrocapsa	aperta	147	115	118	143	145	141	127	110	139	158	175	146	185	167	178	186	182	241
Gephyrocapsa	caribbeanica	2	1	2	4	2	5	4		2	1	3	5		3	3	2	2	3
Gephyrocapsa	ericsonii	11	6	4	12	13	14	15	14	10	9	18	5	15	10	9	10	14	16
Gephyrocapsa	muellerae	4	2	18	23	63	49	49	44	40	33	30	33	13	13	12	16	21	12
Gephyrocapsa	oceanica	9	15	22	25	15	18	24	27	13	10	11	22	11	15	14	21	25	15
Gephyrocapsa	sp.(closed)		2	7	1	1	1		2	7		4	5	3	5	4	4	1	
Small Placolith	(< 2.5um)	120	176	156	118	136	112	117	141	106	114	141	106	132	117	125	96	91	109
Subdominant taxa		45	16	28	53	21	41	62	52	65	61	30	60	43	44	23	44	50	37
	Total	515	501	503	502	501	500	510	521	504	503	507	507	505	501	506	508	507	528
Step2																			
Acanthoica	spp.	6	2		2	1	2	4	2		1	3	1	1	2	3	1	1	1
Calcidiscus	leptoporus	73	82	92	123	100	89	131	96	97	79	78	90	82	74	90	87	78	76
Calciosolenia	murrayi	23	21	22	18	15	9	13	16	14	20	24	7	20	31	23	20	39	40
Ceratolithus	spp.																		
Coccolithus	pelagicus		2	4	5	5	17	2	2	6	6	3	1	2	1	3	2	1	
Discosphaera	tubifera		1			1			1	1	1								
Helicosphaera	carteri	20	20	45	34	70	82	56	22	34	43	28	35	30	31	20	41	7	5
Helicosphaera	pavimentum			1	2		1	1	1	4	3	2		2	1	3			
Neosphaera	coccolithomorpha	30	29	23	34	16	16	13	37	28	31	28	21	22	24	29	31	29	43
Oolithotus	fragilis	69	56	41	45	33	26	33	47	62	59	70	67	79	48	52	48	58	75
Pontosphaera	japonica	2	1	1	2	5	3	2	2	2	1	4	1		3	1		1	1
Pontosphaera	spp.		1	1							1		2		1				
Rhabdosphaera	clavigera	19	9	12	4	11	18	17	17	8	7	8	9	11	14	11	13	15	11
Syracosphaera	spp.	22	21	33	21	22	23	10	25	23	24	20	25	27	33	27	16	22	14
Tetralithoides	quadrilaminata		1					1			1			1		1			
Thoracosphaera	spp.					2					1								
Umbellosphaera	irregularis		1	3	3	3	3	1	2	2	1	8	9	2	12	2	4		2
Umbellosphaera	tenuis	1	5	4	6	2	1	1	4		1	2	5	4	1			1	2
Umbilicosphaera	hulburtiana				1								1	4	4	2	6	9	6
Umbilicosphaera	sibogae	35	52	20	4	14	13	19	28	19	21	25	28	17	20	33	33	41	27
Subdominant taxa	Total	300	304	302	304	300	303	304	302	300	301	303	302	304	300	300	302	302	303
	Reworked specimens	0	2	1	1	1	2	1	1	3	0	0	2	0	3	2	2	0	0

at stage 6 is well correlated, but the reverse occurs for stage 1. The percentage abundance of *R. clavigera* displays numerous fluctuations with no systematic correspondence with the $\delta^{18}O$ record. Percentage values are low in comparison with what is recorded in core RC12-113. *Syracosphaera* spp. are abundant during stages 7 and early 5, and decrease in abundance during stage 6. The percentage values maintain a zigzag pattern from stages 5 to 1, but there is no significant relationship with the $\delta^{18}O$ record. The percentage abundance of *U. irregularis* peaks during stage 7, and shows very low value ($\sim 1\%$) during stages 6 to 1. On the other hand, *U. tenuis* is rare during stages 7 to 2, and shows high values during stage 1; this follows a similar trend found in core RC12-113. The abundance values of *U. irregularis* and *U. tenuis* in core Z-2108 are low when compared to core RC12-113. The percentage abundance of *U. sibogae* increases during interglacial periods and decreases during glacial periods; again, this follows the pattern recognized in core RC12-113.

4.3. Core GC-3 (Table 3)

Core GC-3 is located today near the Subtropical Convergence. The $\delta^{18}O$ of planktonic foraminifera was measured and it is used for stratigraphic correlation. The oxygen isotope curve suggests that 4 glacial–interglacial cycles are represented in this core.

Figs. 4a and b documents the stratigraphic occurrence of dominant and subdominant species in core GC-3, respectively. *E. huxleyi* is abundant from middle stage 5 to stage 1, especially dominant during the Holocene. This increasing trend for *E. huxleyi* upcore near the top is common to all three cores studied. When compared to the occurrences

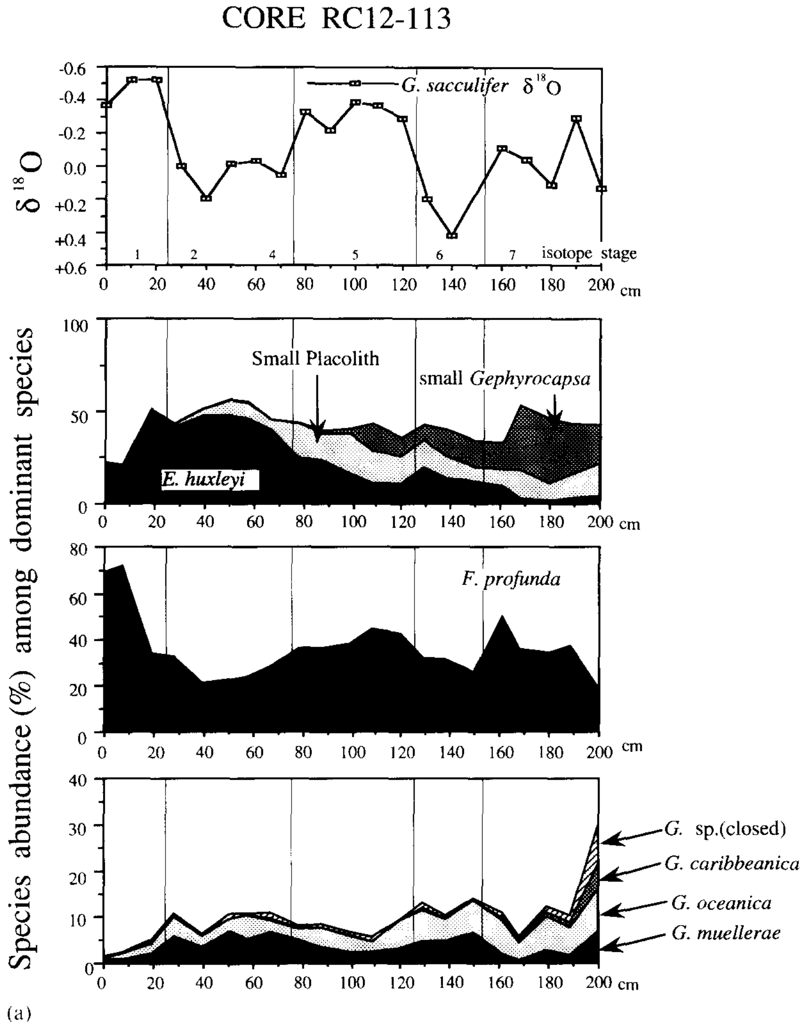

Fig. 2. a. Distribution of the various dominant species of calcareous nannoplankton, presented as percentages in among all dominant taxa, for core RC12-113 compared with the $\delta^{18}O$ record of *G. sacculifer* from Anderson et al. (1989).

b. Distribution of the various subdominant species of calcareous nannoplankton, presented as percentages in among all subdominant taxa, for core RC12-113.

of cores RC12-113 and Z-2108, the bottom horizon of *E. huxleyi* acme interval appears earlier in core GC-3. Small Placolith is abundant during late stage 5 in the former two cores, whereas *E. huxleyi* has already achieved major species status for that same time in core GC-3. Supplementary SEM observations revealed that *E. huxleyi* does not occur in the samples at the depth of 346, 385 and 469 cm. This indicates that the first appearance datum for *E. huxleyi* is definitely represented in core GC-3, and corresponds to a level close to, but above, 346 cm in depth. The occurrences of Small Placolith and small *Gephyrocapsa* in core GC-3 are completely different from those seen in cores RC12-113 and Z-2108, where the shift of the floral dominance from small *Gephrocapsa* — to Small Placolith — to *E. huxleyi* is revealed. In core GC-3, the relationship between all three morphotypes show a seesaw pattern, best observed at early stage 5, stage 7 and stage 10. The first two

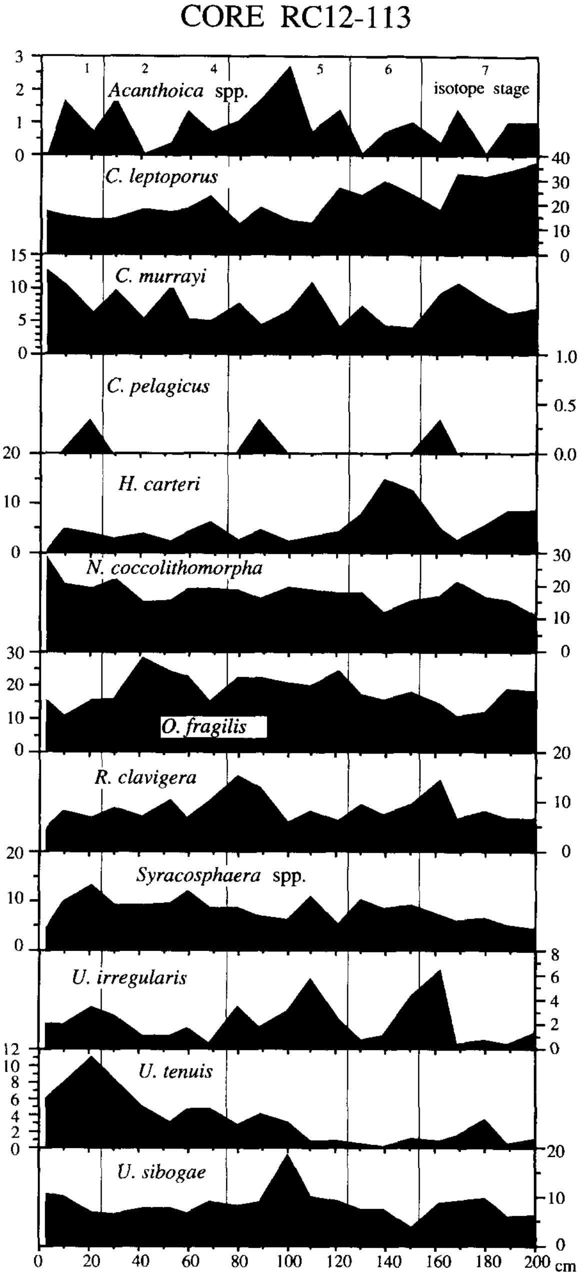

(b)

horizons (peaks) coincide with a major increase in values for *F. profunda*. This correspondence suggests that Small Placolith and small *Gephyrocapsa* invaded higher latitudes, together with low-latitude species, probably resulting from an intensification of the East Australian Current along the eastern side of Tasmania and/or a southern incursion of the STC during interglacial periods. In other words, the distribution of the two small taxa (*Gephyrocapsa* and Small Placolith) is considered to be restricted north of the STC. However, this interpretation cannot explain the occurrence of the same taxa during stage 10, when the percentage of *F. profunda* shows low value. This complicated and unsystematic occurrence of those small taxa indicates that their occurrence may be affected by other environmental factors, presumably suggesting a change in nutrient supply, as well as a water temperature change. The percentage abundance of *F. profunda* in core GC-3 shows low values in comparison with that of cores RC12-113 and Z-2108; this confirms its dominance in low latitudes. Several abundance peaks for this species appear to parallel the $\delta^{18}O$ peaks, except for two peaks which relate to LGM and early stage 8. The genus *Gephyrocapsa* is very abundant in core GC-3 in comparison with the other two cores, especially upon examining the percentage of *G. muellerae* which is extremely high through stages 12 and 11 and stages 6 to 3. Abundant *G. muellerae* occur with Small Placolith, small *Gephyrocapsa* and *Gephyrocapsa* sp. (closed) during stages 10 to 7. From stage 3 to the Recent, the percentage of *G. muellerae* decreases in abundance, and the floral dominance changes to *E. huxleyi*. *Gephyrocapsa* sp. (closed) is abundant during stages 10 to 8. *G. caribbeanica* shows a similar stratigraphic occurrence to the previous species, but its percentage is low. As mentioned previously in the taxonomic notes, *G.* sp. (closed) is considered to be a calcified form of *G. caribbeanica*, whose central opening is filled in, simply because of the similarity in their stratigraphic occurrence and overall morphology. *G. oceanica*, on the other hand, is rare throughout core GC-3.

The assemblage of the subdominant species in core GC-3 is characterized by the dominance of *C. leptoporus*, *C. pelagicus* and *H. carteri*, whereas the percentage abundances of middle- to low-latitude species such as *Acanthoica* spp., *C. murrayi*, *N. coccolithomorpha*, *O. fragilis*, *R. clavigera*, *Syracosphaera* spp., *U. irregularis*, *U. tenuis* and *U. sibogae* display low values. The percentage

Table 3

Species occurrence chart for all species recovered in core GC-3

GC-3 (1/3)	Sample Depth (cm)	0-1	5-6	10-11	15-16	20-21	25-26	30-31	35-36	40-41	45-46	50-51	55-56	60-61	65-66	71-72	75-76	80-81	85-86	90-91	95-96	100-101	105-106	110-111	115-116	120-121	125-126	130-131	135-136	140-141	145-146	150-151	155-156	160-161
Abundance		A	A	A	A	A	A	A	A	A	A	A	A	A	A	A	A	A	A	A	A	A	A	A	A	A	A	A	A	A	A	A	A	A
Preservation	perfect C. lepto. %	38	63	47	53	40	46	60	35	30	31	39	42	38	43	22	34	52	39	35	34	40	31	31	26	40	37	59	55	45	50	59	49	44
Step 1																																		
Emiliania	huxleyi	404	384	409	298	313	238	225	217	329	249	118	138	240	150	150	128	120	219	263	201	171	115	141	103	82	101	99	58	27	48	17	20	9
Florisphaera	profunda	21	7	15	22	18	12	5	36	11	10	9	12	6	10	9	7	9	5	8	8	7	6	18	8	16	9	20	35	8	3	4	6	3
Gephyrocapsa	aperta		2				2	3	3			1	1	3	1	1	2		5	3	4	5	5	14	4	6	7	9	82	21	10	8	10	2
Gephyrocapsa	caribbeanica			1																														
Gephyrocapsa	ericsonii	1		1		2	1	2						1						4		7	2	14	9	13	12	12	10	21	15	4	8	5
Gephyrocapsa	muellerae	21	38	34	117	115	141	180	221	151	231	372	349	246	361	329	419	354	253	205	298	286	356	304	363	339	380	333	239	366	454	467	446	471
Gephyrocapsa	oceanica	8	14	7	18	8	4	5	2			1	1	1	2			2	1	1	4	2	4		1	6	1	9	5	2	1			1
Gephyrocapsa	protohuxleyi																																	
Gephyrocapsa	sp.(closed)	8	8	8	4	2	7	4	10	1	2	8	5	3	10	7	7	6	1	3	3	2	5	5	3	4	5	2	7	15	4	4	6	10
Small Placolith	(< 2.5um)	3	7	9	4	7	12	5	5	4	17	4	4	15	6	6	7	7	11	6	8	11	7	16	5	9	13	12	65	18	15	6	7	2
Subdominant taxa		47	66	38	44	51	99	84	24	13	9	3	3	7	15	10	8	11	20	18	15	23	12	16	35	42	12	32	11	44	3	16	4	11
	Total	513	526	522	507	516	516	513	518	509	518	516	513	522	555	512	578	509	515	511	541	514	512	528	531	517	540	528	512	522	553	526	507	514
Step2																																		
Acanthoica	spp.			1																1								1						
Calcidiscus	leptoporus	223	209	228	185	184	127	152	145	60	111	167	170	61	144	94	85	132	152	161	177	167	167	184	184	154	197	173	194	177	206	118	165	146
Calciosolenia	murrayi	1		7	5	1					1		1	1	1		1	1		1							4	1	7	2	7	2	10	2
Ceratolithus	spp.													1																				
Coccolithus	pelagicus	23	23	9	6	28	118	122	90	189	143	94	48	198	73	172	150	66	44	18	45	44	50	38	22	36	11	6	12	55	20	153	95	108
Coccolithus	streckerii	1	1				1	1	1	2	2			3	1	4	1		1	1	1	1	3	1			1	2			1	7	4	5
Helicosphaera	carteri	31	46	16	20	41	34	16	43	40	30	25	33	25	47	18	44	50	68	102	59	53	64	68	81	95	55	55	20	64	38	21	13	25
Helicosphaera	inversa																																	
Helicosphaera	pavimentum				1								1																		1			
Neosphaera	coccolithomorpha	6	4	12	19	4	3	1	4	1	1	3	5	2	3	2	1	7	6	1		3		1	1	4	4	9	5		3			3
Oolithotus	fragilis	9	11	15	14	12	2	3	3	1	2	2	7	3	13	3	8	30	20	7	6	26	9	8	6	11	17	50	49	10	11		1	3
Pontosphaera	japonica			1						1					1		1	1				1												
Pontosphaera	multipora										1																							
Rhabdosphaera	clavigera			4	7	4	1		3	1	3	2	10	1	4	4	3	3	5	1	4	3	5	3	1	6	6	6	2	4	5	2	6	7
Syracosphaera	spp.	3	8	2	15	7	6	4	3	3	1	1	11	1	5		2	1	4	3		2	1	1	1		4	2	6	1	2		3	
Tetralithoides	quadrilaminata												1																					
Umbellosphaera	irregularis		1															1						1									1	
Umbellosphaera	tenuis	1		4	1										1																			
Umbilicosphaera	sibogae	3	4	4	28	22	8	2	8	2	5	6	13	7	13	3	8	17	3	5	11	7	7	1	4	4	3	5	14	4	6	1	7	7
Subdominant taxa	Total	301	307	303	301	303	300	301	300	300	300	300	300	303	306	300	304	309	303	301	303	307	306	306	300	310	302	310	309	317	300	304	305	306
	Reworked specimens	1	1	1	0	0	3	2	4	2	2	1	1	0	0	1	1	1	2	1	1	1	0	1	1	1	1	0	0	0	1	0	0	0

GC-3 (2/3)	Sample Depth (cm)	165-166	168-169	172-173	175-176	180-181	185-186	190-191	195-196	200-201	205-206	210-211	215-216	220-221	225-226	230-231	235-236	240-241	245-246	250-251	255-256	262-263	265-266	270-271	275-276	280-281	285-286	290-291	295-296	300-301	305-306	310-311	315-316	320-321
Abundance		A	A	A	A	A	A	A	A	A	A	A	A	A	A	A	A	A	A	A	A	A	A	A	A	A	A	A	A	A	A	A	A	A
Preservation	perfect C. lepto. %	49	46	40	36	20	41	39	22	27	20	29	14	16	30	31	39	51	46	27	27	21	11	18	15	17	32	16	27	19	6	13	18	16
Step 1																																		
Emiliania	huxleyi	17	19	29	29	27	36	37	34	39	49	10	27	23	42	91	114	54	81	43	5	3	9	8	10	13	5	1	5	10	14	17	7	7
Florisphaera	profunda	7	6	9	4	9	13	17	22	29	40	42	58	27	28	28	32	19	21	21	12	6	28	38	7	7	1	5	1	3	4	10	2	16
Gephyrocapsa	aperta	9	7	10	3	7	12	8	6	24	50	165	203	187	74	81	84	111	35	40	14	2	6	12	15	21	10	13	30	14	27	30	13	37
Gephyrocapsa	caribbeanica														2	4	7	10	24	17	32	26	26	21	27	21	16	17	32	23	22	17	20	23
Gephyrocapsa	ericsonii	18	12	8	6	9	21	15	8	20	26	23	31	24	12	8	12	8	3	3	6	1		1		1	2	3	6	8	6	7	6	4
Gephyrocapsa	muellerae	448	458	455	455	441	398	424	407	352	205	70	52	91	269	161	85	68	95	128	178	165	212	196	175	153	130	134	144	138	179	141	140	159
Gephyrocapsa	oceanica	2	2	3	1		1	2	3	1	13	12	2	3	11	5	2	4	6	3	4	4	2	3	3	2	1	2	2	1	3	1	3	1
Gephyrocapsa	protohuxleyi																																	
Gephyrocapsa	sp.(closed)	15	10	10	7	10	4	2	1	5	15	16	8	8	11	38	36	98	160	181	228	271	219	202	226	270	318	304	260	276	247	240	291	226
Small Placolith	(< 2.5um)	5	4	6	1	4	3	6	3	13	27	85	128	137	42	77	121	111	27	37	16	2	8	19	22	16	15	9	31	14	21	38	14	28
Subdominant taxa		2	15	8	4	8	21	9	20	18	76	83	3	6	31	16	17	25	48	31	9	29	7	11	27	5	12	18	3	17	4	6	8	11
	Total	523	533	538	510	515	509	520	504	501	501	506	512	506	522	509	510	508	500	504	504	509	517	511	512	509	510	506	514	504	527	507	504	512
Step 2																																		
Acanthoica	spp.														1											1	1	1						
Calcidiscus	leptoporus	196	138	141	141	84	165	178	171	155	74	139	227	213	200	164	165	154	144	48	105	53	86	98	83	103	135	140	144	111	116	118	197	201
Calciosolenia	murrayi	1	1		2	1	1						1	1	3	2		1	2	1							1			1	1		2	1
Ceratolithus	spp.														1																			
Coccolithus	pelagicus	53	73	71	60	131	59	60	72	73	187	131	17	13	35	71	42	35	102	228	132	214	182	144	176	138	70	84	108	133	136	127	54	39
Coccolithus	streckerii		1	1	1			1			1	2				2			2	4	8	2	1	4	2	2	2	4	4	2	1	4	3	
Helicosphaera	carteri	27	62	61	62	67	62	48	29	36	33	28	21	23	23	29	22	42	28	12	27	32	24	47	43	56	74	49	35	44	35	31	27	32
Helicosphaera	inversa																																	
Helicosphaera	pavimentum																																	
Neosphaera	coccolithomorpha	2	1	4	9	5	3	3	4	9	1		1	5	3	1	4	4	2		3	1	2	2	1	2	2	2	1	1	1	2	2	4
Oolithotus	fragilis	4	3	5	7	4	9	5	5	13	3	6	15	13	15	18	50	53	13	5	10	1	1	1	1	5	14	8	6	5	8	12	7	17
Pontosphaera	japonica	1	4	2		1			1	1		1			1		1					1		1										
Pontosphaera	multipora																																	
Rhabdosphaera	clavigera	6	3	1	5	3	3	1	4	2	4		4	7	7	5	5	6	2	3	5	3	3	5	1	1	1	3	1		4	4	3	4
Syracosphaera	spp.	5	5	5	4	1	4	3	1	6	2	2	1	6	2		4	9	5	1	1			2	2	2	6	9	7	4	6	2	3	4
Tetralithoides	quadrilaminata						1														1													
Umbellosphaera	irregularis	1													1																			
Umbellosphaera	tenuis										1					2																		
Umbilicosphaera	sibogae	5	14	11	10	3	5	3	13	17	7	10	15	20	15	10	13	9	2	1	8	2	1	3	3		5	2	4	2	5	3	3	2
Subdominant taxa	Total	301	305	302	301	300	312	302	300	312	313	319	302	301	307	304	306	313	302	303	300	309	300	307	312	310	311	302	310	303	313	303	301	304
	Reworked specimens	2	4	1	0	2	1	0	1	2	1	4	0	0	2	2	1	1	1	1	4	3	4	1	3	2	4	5	6	4	3	1	4	0

GC-3 (3/3)	Sample Depth (cm)	325-326	330-331	335-336	340-341	344-345	346-347	350-351	355-356	360-361	365-366	370-371	373-374	377-378	380-381	385-386	390-391	395-396	400-401	405-406	410-411	415-416	420-421	425-426	430-431	435-436	440-441	445-446	450-451	455-456	460-461	465-466	469-470
Abundance		A	A	A	A	A	A	A	A	A	A	A	A	A	A	A	A	A	A	A	A	A	A	A	A	A	A	A	A	A	A	A	A
Preservation	perfect C. lepto. %	21	21	32	27	41	40	43	28	22	36	18	24	24	15	17	25	36	30	15	16	19	21	32	37	50	38	45	30	25	33	23	39
Step 1																																	
Emiliania	huxleyi	3	3	2	4	1	64	25	19	27	29	24	17	24	37	48	15	37	18	14	23	7	22	32	63	47	52	42	13	15	14	13	30
Florisphaera	profunda	12	15	9	11	6	7	6	2	5	7	13	10	4	5	10	3	5	3	3	5	6	3	4	14	23	23	15	11	10	7	2	15
Gephyrocapsa	aperta	68	50	73	62	79	99	63	50	41	101	103	122	106	112	103	64	105	83	37	85	42	59	26	3	2	1	1	2	1			
Gephyrocapsa	caribbeanica	21	14	23	30	23	17	24	16	29	13	10	14	25	14	12	12	13	19	12	18	18	19	28	1	3	4		2	1	5	4	2
Gephyrocapsa	ericsonii	4	1	1	4	1	5	1			5	1	1		1	4		2				1		1									
Gephyrocapsa	muellerae	133	137	145	142	131	147	139	161	190	129	152	112	120	148	120	166	122	178	210	154	206	194	250	356	375	335	349	402	453	447	473	438
Gephyrocapsa	oceanica	2	1		1		2		1	1				1	1	1			2		1			4	7	9	11	21	4	3	1		2
Gephyrocapsa	protohuxleyi											3			2		1	1				1	1						1				
Gephyrocapsa	sp.(closed)	230	211	205	190	159	123	160	179	169	101	105	92	132	106	92	169	106	129	186	124	192	126	111	34	17	4	4	11	5	10	6	3
Small Placolith	(< 2.5um)	51	63	72	56	101	46	64	55	41	118	95	147	103	101	115	68	116	73	53	98	54	79	34	34	9	9	5	5	2	6	1	8
Subdominant taxa		5	7	17	2	11	6	26	31	9	1	6	1	1	2	1	11	3	4	11	6	3	3	29	30	53	61	63	49	19	15	7	7
	Total	529	502	547	502	512	516	508	514	512	504	512	516	516	529	506	509	510	509	526	514	530	506	519	542	538	500	500	500	509	505	506	505
Step 2																																	
Acanthoica	spp.				1	4						1		2	1				2	1					1			1					
Calcidiscus	leptoporus	219	179	155	161	168	16	39	69	120	111	64	41	77	57	67	66	127	125	119	167	216	187	198	210	196	161	177	212	168	115	92	150
Calciosolenia	murrayi		5	1	3	15	1	1		1	3	4	2	1	2	1	2	3	4	5	5	2	1	1			2						
Ceratolithus	spp.											1							1														
Coccolithus	pelagicus	31	54	103	62	27	271	241	192	145	107	182	230	151	198	179	167	123	99	139	80	29	66	31	14	26	63	33	54	73	124	155	58
Coccolithus	streckerii		2	2	1		2	1	7	1		2	2	5	3	3	4	1	2		1	2	1	1					1		2		
Helicosphaera	carteri	18	23	18	21	18	5	5	16	21	40	33	19	38	28	36	46	38	46	22	24	33	27	51	47	46	43	49	14	39	39	34	68
Helicosphaera	inversa						+	+			+	+		1	+	+	1	1	+	+	1	+	2	+									
Helicosphaera	pavimentum										1							1			1	1											
Neosphaera	coccolithomorpha	5	5	3	5	2	1	1	1		4			1	1	2	4		1	1	3		2	3	4	6	5	6			2	4	1
Oolithotus	fragilis	18	22	8	19	38	3	7	5	3	5	1		1	2	4	3	9	5	7	3	5	6	8	8	8	7	13	3	1	2	5	7
Pontosphaera	japonica			1	3	2				1													1	1						1			1
Pontosphaera	multipora													1																1			
Rhabdosphaera	clavigera	2	4	4	11	5	2		2	1	4	3		6	4	3	1	1	3	1	1		3	2	3	3	2	6	5	1	3	2	9
Syracosphaera	spp.	1	8	6	12	19	4	4	8	9	28	11	6	18	7	4	8	9	12	7	12	8	5	3	8	12	10	8	9	5	2		2
Tetralithoides	quadrilaminata	1																															
Umbellosphaera	irregularis	2				2		1	1									1													1		
Umbellosphaera	tenuis																													1			
Umbilicosphaera	sibogae	6	7	3	1	3	2		3	2	5	1	2	2	1	1	1	2	2		2	4	1	5	7	8	15	16	5	11	11	10	5
Subdominant taxa	Total	303	309	304	300	303	307	300	304	304	308	303	302	304	304	300	303	316	302	302	300	300	302	304	302	305	308	309	303	301	301	302	301
	Reworked specimens	2	1	1	1	0	1	2	1	4	2	3	2	2	0	1	3	2	3	0	5	2	2	2	1	2	2	0	5	4	1	7	2

abundance of *C. leptoporus* increases during interglacial periods, whereas that of *C. pelagicus* increases during glacial periods. The study of modern calcareous nannoplankton distribution in the Tasman Sea (Hiramatsu and De Deckker, 1997-this issue) showed that *C. leptoporus* and *C. pelagicus* are abundant at high latitudes. However, the percentages abundances of both species show a reverse relationship, thus implying that these taxa must either complement each other or compete for the same ecological niche. Nevertheless, it appears that *C. pelagicus* occurs in large numbers during the low TN values (viz. low temperature). The high values of *C. leptoporus* could indicate high-productivity events following the characteristics of this species given by Roth and Berger (1975, table 1). The percentage abundance of *H. carteri* does not show a systematic relationship with the $\delta^{18}O$ record. *H. carteri* is apparently abundant during stage 5 in core GC-3 but, on the other hand, the percentage of this species shows low value at the same stage in cores RC12-113 and Z-2108. The percentage abundance of *U. sibogae* displays peaks during interglacial periods, but it is not obvious at stages 5 and 9.

The occurrences of biostratigraphic indicators throughout this core are reported below. *Helicosphaera inversa* is very rare, but constantly occurs during stage 10. This occurrence seems to be stratigraphically restricted. Takayama and Sato (1987) reported that the first and last occurrences of *H. inversa* are dated at 0.48 and 0.15 Ma, respectively, in the north Atlantic Ocean. Matsuoka and Okada (1989) reported that this species continuously occurs for the period ranging from 0.80 to 0.54 Ma in the northwestern Pacific Ocean. *H. inversa* was not found in cores RC12-113 and Z-2108. The last occurrence of *Pseudoemiliania*

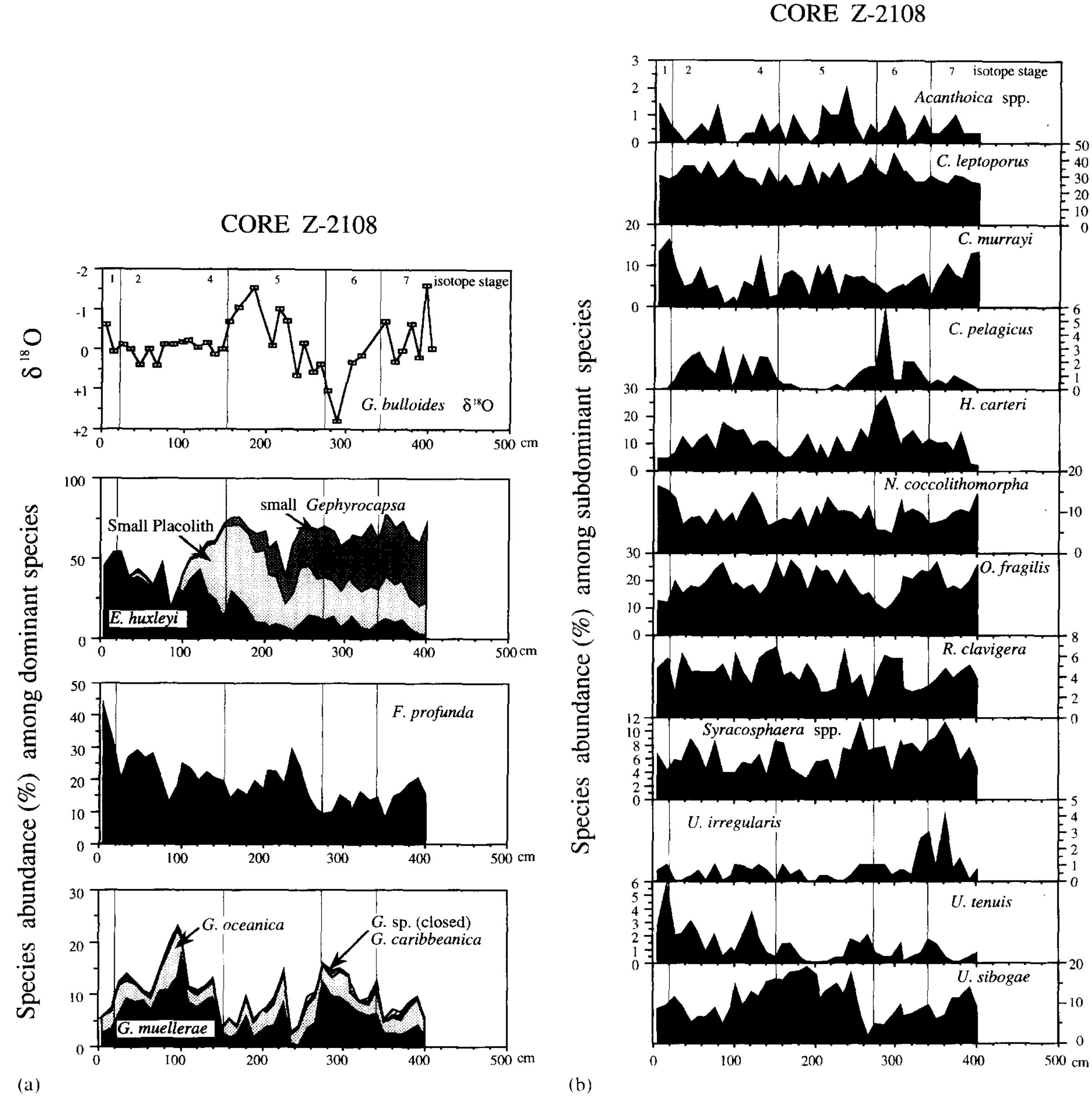

Fig. 3. a. Distribution of the various dominant species of calcareous nannoplankton, presented as percentages in among all dominant taxa, for core Z-2108 compared with the $\delta^{18}O$ record of *G. bulloides* from Nelson et al. (1993).

b. Distribution of the various subdominant species of calcareous nannoplankton, presented as percentages in among all subdominant taxa, for core Z-2108.

lacunosa, which is regarded as a useful biostratigraphic marker dated 0.458 Ma by Thierstein et al. (1977), is not recognized in this core. The oxygen isotope data suggest that the disappearance horizon of this species could be correlated to just below of the bottom of core GC-3.

5. Estimates of palaeo-SST based on recent calcareous nannoplankton assemblages

The distribution of numerous calcareous nannoplankton species recovered from core-top sediments in the Tasman Sea is strongly controlled by SST (Hiramatsu and De Deckker, 1997-this issue). This suggests that an estimate of palaeo-SST using the nannofloral composition from core samples ought to be feasible. Following on from the study of calcareous nannoplankton from 53 core-top samples from the Tasman and Coral Seas, a ratio could be established to compare summer SST and a combination of subdominant taxa: $W/(W+C)$.

W representing the total percentage of species mainly distributed in middle to low latitudes (*Acanthoica* spp., *C. murrayi*, *D. tubifera*, *N. coccolithomorpha*, *O. fragilis*, *R. clavigera*, *Syracosphaera* spp., *U. irregularis*, *U. tenuis* and *U. sibogae*), and C representing the percentage of species dominating at high latitudes (*C. leptoporus* and *C. pelagicus*). This ratio $W/(W+C)$ is plotted against SST in Fig. 5. Data of poorly preserved samples taken from deep-sea floor, and data of samples collected near the equatorial region, where *C. leptoporus* is regarded as low-latitude species, have been eliminated from this figure. As a consequence, only 43 data points were plotted in Fig. 5. The value of this ratio is well correlated with SST [correlation coefficient $r^2=0.905$]. Thus, this ratio directly related to SST, has been applied to the core data to estimate palaeo-SST based on the change of $W/(W+C)$ ratio through time.

The estimated palaeo-SST tentatively, named as TN here, shows a good correspondence with the $\delta^{18}O$ records in all three cores (Fig. 6). The TN curves obviously related to glacial–interglacial cycles.

The conventional method for the palaeotemperature estimation by using the ratio of warm and cold species is rather easy to carry out and can thus become a useful tool for rapidly determining climatic trends as reflected in cores. However, as discussed in detail by Yanagisawa (1993), this value is sensitive as a reliable thermometer *only* within a region of mixed water masses, whereas the palaeotemperature fluctuation signals are easily deformed in regions affected by a warm or cold current. Moreover, it is obvious that the TN value used here is insensitive to SST below 12°C, due to the lack of recent core-top data (Hiramatsu and De Deckker, 1997-this issue) for nannoplankton living at temperatures below 12°C (Figs. 5 and 6). As a consequence, there became a need to develop here another method relying, in this case, on a statistical package in an attempt to estimate palaeo-SST.

According to Hiramatsu and De Deckker (1997-this issue), the percentage abundances of *Emiliania huxleyi*, *Florisphaera profunda* and *Calcidiscus leptoporus* are well correlated with SST in the Tasman Sea today. It is considered, therefore, that these species ought to be useful indicators for palaeo-SST. Unfortunately, the abundance of *E. huxleyi* drastically changes near the stages 4 and 5 boundary, and abundance values are very low for levels below stage 4. Obviously, this trend does not represent a temperature change, but a phylogenetic change instead, as exemplified by *E. huxleyi* displaying a different pattern from the $\delta^{18}O$ and TN curves. In other words, the relationship between the percentage of *E. huxleyi* and SST after the stages 4 and 5 boundary differs from before and, therefore, the modern relationship between the percentage abundance of *E. huxleyi* and SST cannot be applied to those strata older than the *E. huxleyi* acme Zone (Gartner, 1977) for estimating past SST. The occurrence of *F. profunda* in deep-sea cores, and which is occurs in the lower photic zone (Okada and Honjo, 1973), again is not directly related to SST. However, there is the apparent broad relation that is recognized between the low percentage values of *F. profunda* and the dissolution index using *C. leptoporus*. The pattern or movement of the Turbulent Boundary Layer in the upper ocean that affects *F. profunda*, following Molfino and McIntyre's (1990a,b) observations for the tropical Atlantic Ocean, is not clear in the case of core GC-3 because other factors, apart from temperature, must control the abundance of *F. profunda*. According to the distribution of *C. leptoporus* in surface sediments in the Tasman Sea (Hiramatsu and De Deckker, 1997-this issue), the percentage abundance of this species increases towards high latitudes, but high values are also shown in the equatorial region. This result suggests

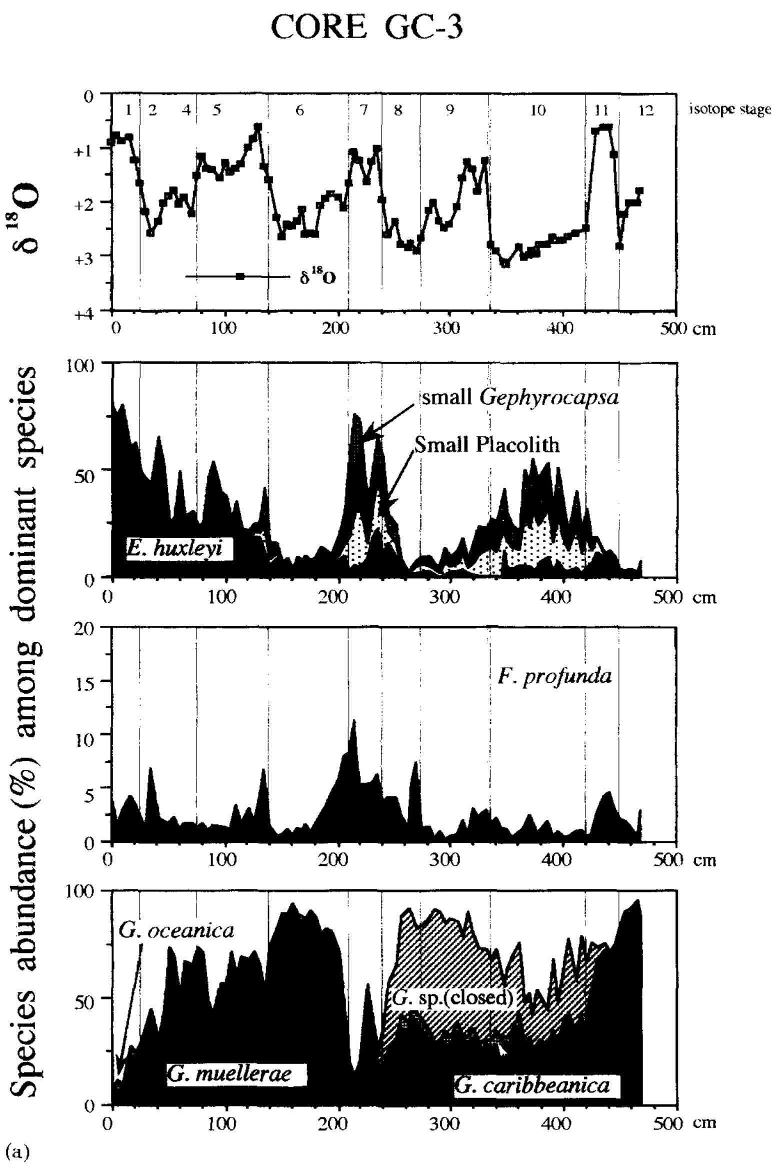

Fig. 4. a. Distribution of the various dominant calcareous nannoplankton species, presented as percentages in among all dominant taxa, for core GC-3 compared with the $\delta^{18}O$ record of *G. bulloides* (for further details see text).

b. Distribution of the various subdominant calcareous nannoplankton species, presented as percentages in among all subdominant taxa, for core GC-3.

again that the percentage abundance of *C. leptoporus* is not only affected by SST, but very likely by another factor such as the availability of nutrients as was identified already by Roth and Berger (1975). Additional information is provided in Hiramatsu and De Deckker (1997-this issue).

To sum up the above, it is difficult to postulate a palaeo-SST with great precision and confidence, by simply using the relationship between the percentage abundance of a single species and SST, especially by looking at *F. profunda*, *C. leptoporus* and *E. huxleyi*, either together or separately. The

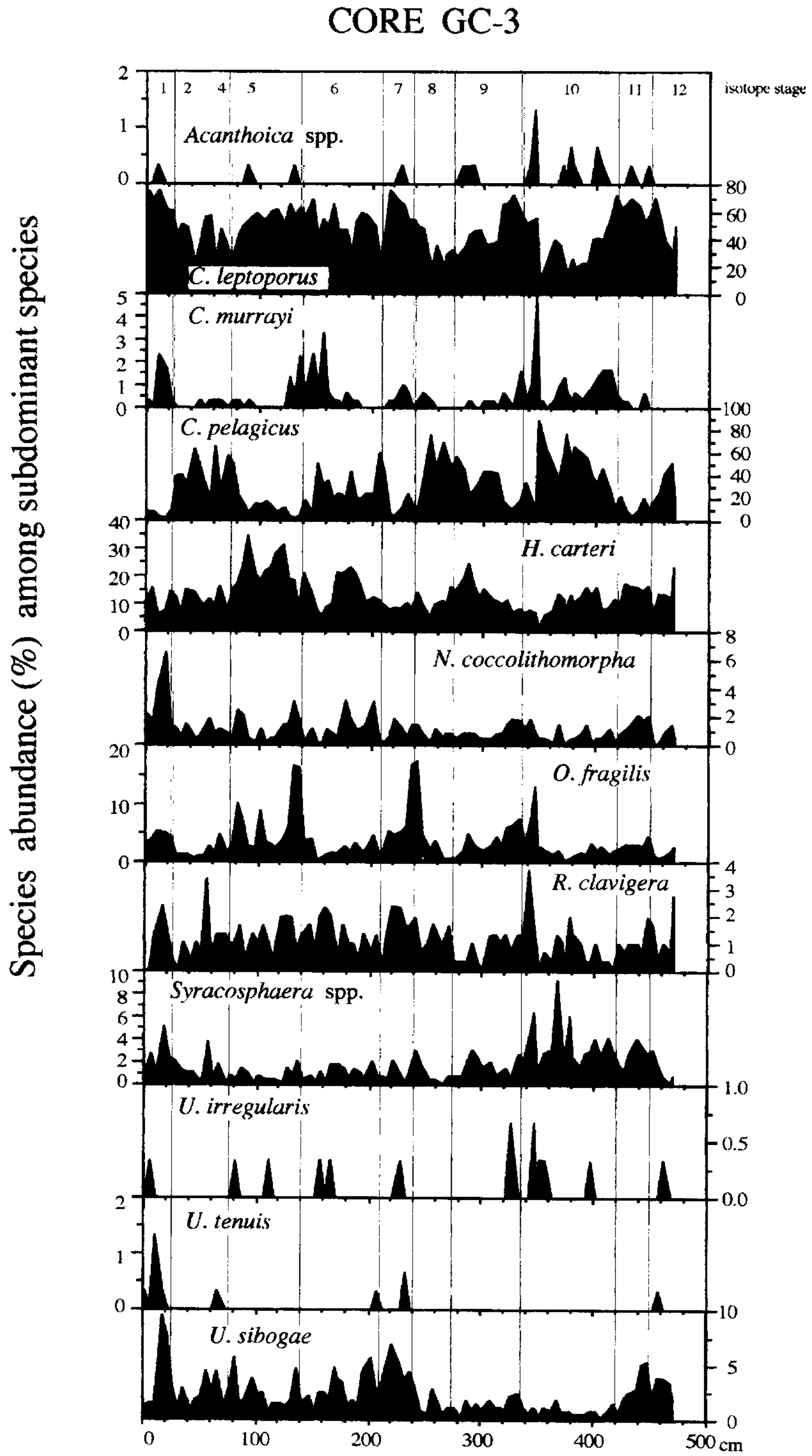
CORE GC-3
isotope stage
1 2 4 5 6 7 8 9 10 11 12
Species abundance (%) among subdominant species
Acanthoica spp.
C. leptoporus
C. murrayi
C. pelagicus
H. carteri
N. coccolithomorpha
O. fragilis
R. clavigera
Syracosphaera spp.
U. irregularis
U. tenuis
U. sibogae
0 100 200 300 400 500 cm

(b)

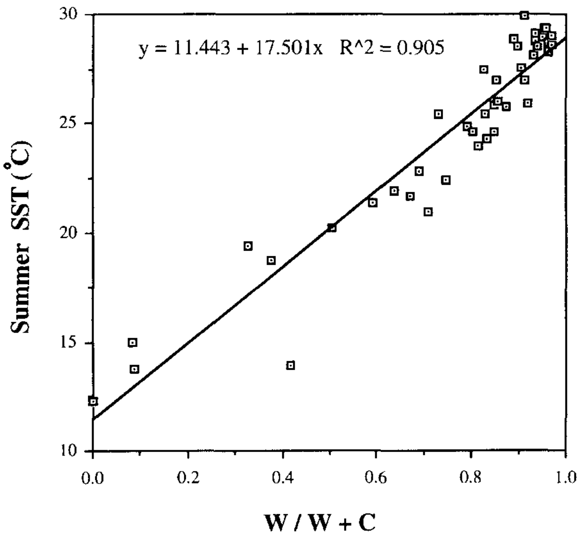

Fig. 5. Relationship between $W/(W+C)$ and sea-surface temperature, where W represents the percentage of species principally distributed in middle to low latitudes, and C represents those species dominating at high latitudes.

next approach, viz. to use a transfer function was also tried through reference of the assemblages data, and through a combination of selected species which are relatively well correlated with SST; all these species are recovered from the core-top sediments samples studied by Hiramatsu and De Deckker (1997-this issue). Two data sets involving all species including the dominant species, as well as subdominant species in the first instance, and only through use of a combination of *F. profunda* and *G. muellerae*, and combination of *C. leptoporus*, *N. coccolithomorpha*, *O. fragilis* and *U. sibogae*, (for all 3 cores) and *C. pelagicus* (for core GC-3) were treated with the Principal Coordinate Analysis Statistical Package GENSTAT 5 in an attempt to develop a transfer function [for further discussion refer to Hiramatsu and De Deckker (1997-this issue)]. Unfortunately, in all cases, no obvious correlation could be made between scores of recent data and those of core data, implying that additional environmental information (e.g., perhaps nutrients, dissolved oxygen) is required for the modern data set before coming up with a useful transfer function.

6. $CaCO_3$ dissolution patterns

Although the dissolution of coccoliths had been investigated quite extensively through the works of Honjo (1975) and Roth and Berger (1975), it is the method of Matsuoka (1990) which provided a means of evaluating the degree of $CaCO_3$ dissolution. Matsuoka's (1990) method involves measuring the ratio of the perfectly preserved to the broken/partly dissolved coccoliths of *Calcidiscus leptoporus*. This method is applied herewith to the three cores to investigate the change in degree of dissolution through time, and determine the relationship between the dissolution curves and the $\delta^{18}O$ record in the three cores. Up to 100 specimens of *C. leptoporus* were counted for each sample under a microscope at 1600× magnification. The well-preserved specimens are called herein "perfect *C. leptoporus*".

The percentage of perfect *C. leptoporus* is compared against the $\delta^{18}O$ value for three cores in Fig. 7. The percentage of perfect *C. leptoporus* in core RC12-113 maintains a high value, mostly within the range of 50–70% except for one low value during stage 7. This percentage does not show a systematic relationship with the $\delta^{18}O$ value in core RC12-113. The percentage values of perfect *C. leptoporus* in core Z-2108 are also fairly high (mostly 45–65%) and show many short-term fluctuations. Again, the percentage values do not show a systematic relationship with the $\delta^{18}O$ value. As mentioned earlier, only a small amount of sediment preserved inside the *Orbulina universa* foraminifers was used for the nannoplankton study only for each level in core Z-2108. This procedure appears not to affect the estimates of *C. leptoporus* preservation since there is no significant difference in the degree of preservation/dissolution between the two cores RC12-113 and Z-2108. Of interest, however, are the apparent high values of perfect *C. leptoporus* in the vicinity of the stages 5e–6 boundary in both cores. This phenomenon is repeated at the stages 1–2 transition. Nannoplankton specimens in core GC-3 are much more affected by dissolution in comparison with the other two cores. The percentage of perfect *C. leptoporus* ranges from 10% to 60%, but is usually less than 50%. There are intricate relationships between this percentage

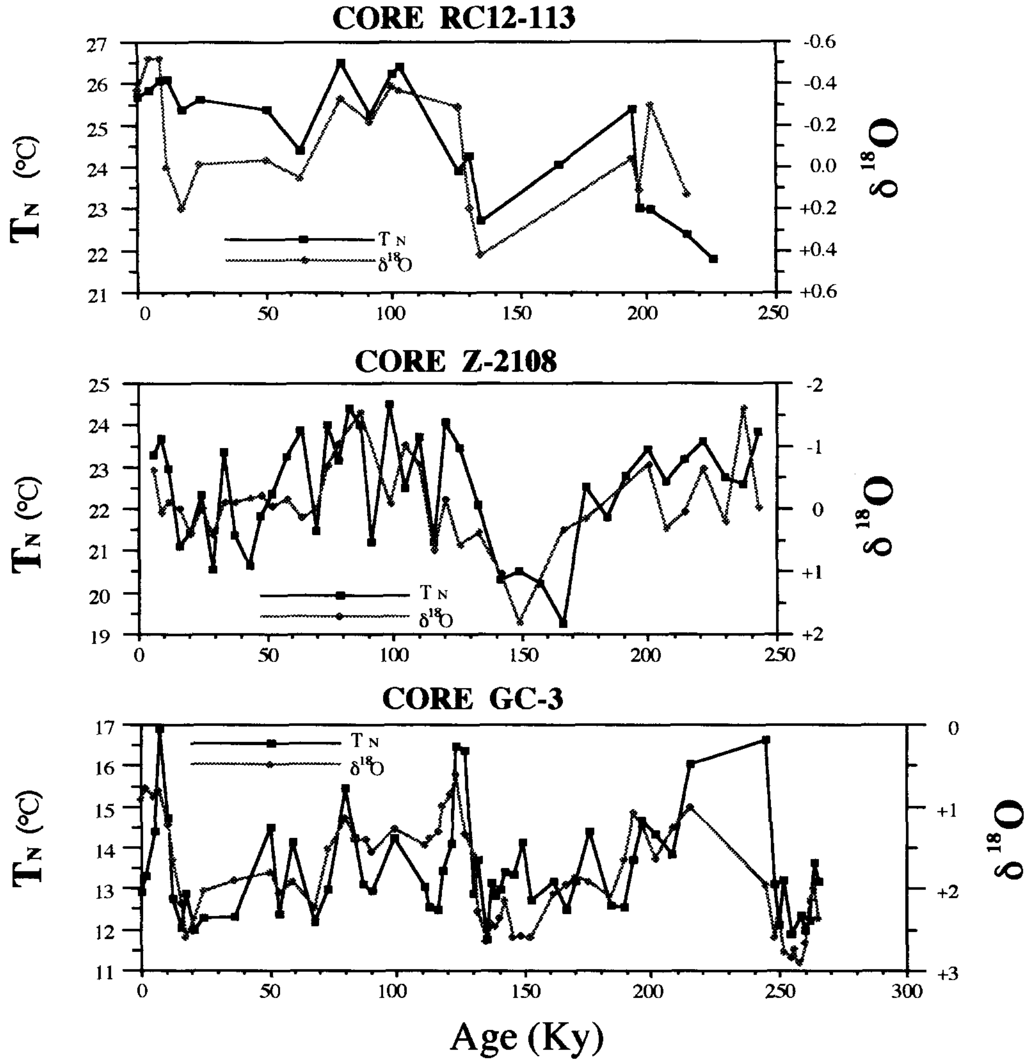

Fig. 6. $\delta^{18}O$ record and sea-surface temperatures equated to TN being established through a combination of nannoplankton taxa for cores RC12-113, Z-2108 and GC-3 (for further details see text).

and the $\delta^{18}O$ record. During stage 11, both peaks correspond well. However, during other interglacial periods, they do not show a good correspondence. Again, preservation values are higher at the glacial–interglacial boundaries or at the end of glacial periods in core GC-3.

The reason for this correspondence between the percentage of perfect *C. leptoporus* and the $\delta^{18}O$ record in core GC-3 cannot be interpreted successfully at this stage. This might be related to the amount of dissolved CO_2 at the ocean floor near the Subtropical Convergence. If so, this could relate to the amount of CO_2 in the atmosphere and the intensification of winds and ocean current systems which control the intensification of the downwelling process, pumping dissolved CO_2 from sea-surface.

7. Conclusions

(1) A temperature-related ratio of calcareous nannoplankton TN: $[W/(W+C)]$ based on the modern-day distribution of selected species

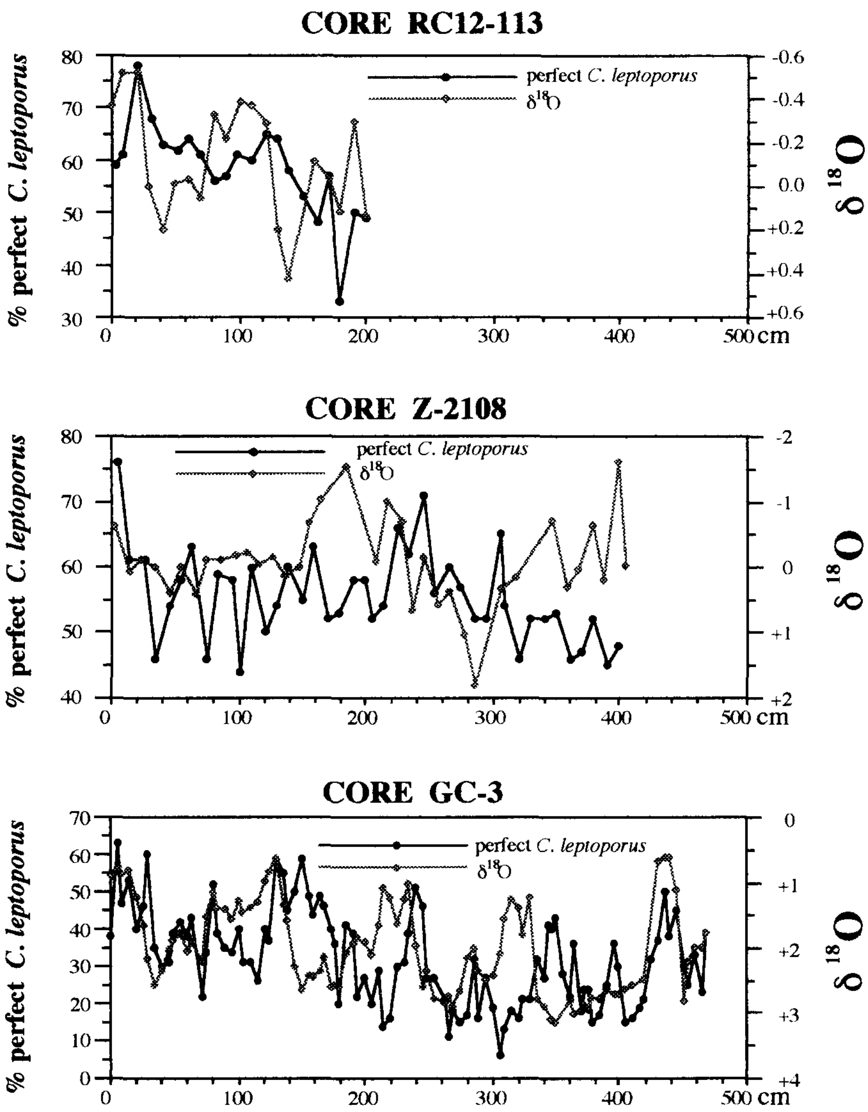

Fig. 7. $CaCO_3$ dissolution patterns in the three cores, evaluated through the ratio of "perfect *Calcidiscus leptoporus*" (for further details see text).

(*W*: *Acanthoica* spp., *Calciosolenia murrayi*, *Discosphaera tubifera*, *Neosphaera coccolithomorpha*, *Oolithotus fragilis*, *Rhabdosphaera clavigera*, *Syracosphaera* spp., *Umbellosphaera irregularis*, *U. tenuis* and *Umbilicosphaera sibogae*; and *C*: *Calcidiscus leptoporus* and *Coccolithus pelagicus*) was developed and applied to the three cores from the Tasman Sea. The TN value shows a good correspondence with the $\delta^{18}O$ record in three cores.

(2) The calcareous nannoplankton composition of all three cores was studied, and the relationships between the percentage abundance of each species and the $\delta^{18}O$ record of planktonic foraminifers are presented.

(3) The shift from small *Gephyrocapsa* — to Small

Placolith — to *Emiliania huxleyi* is recognized in cores RC12-113 and Z-2108, but the occurrences of the two former taxa show alternating patterns in core GC-3. This biostratigraphic indicator is useful for identifying isotope stages 4 and 5 for middle latitudes in the Tasman Sea, but the southern extent of this phenomenon occurs at the Subtropical Convergence.

(4) *Gephyrocapsa muellerae* increased its geographical abundance southward and stratigraphically during glacial periods, whereas *Florisphaera profunda* showed a reverse relationship. *C. pelagicus* increased its abundance southwards, and particularly so during glacial periods. In contrast, *U. sibogae* increases northward, especially during interglacial periods. *C. leptoporus* and *Helicosphaera carteri* geographically increase southward, and *Acanthoica* spp., *C. murrayi*, *N. coccolithomorpha*, *O. fragilis*, *R. clavigera*, *Syracosphaera* spp., *U. irregularis* and *U. tenuis* can increase northward from their present-day occurrences as seen in all three cores. However, these taxa do not clearly show systematic correspondence with the $\delta^{18}O$ record.

(5) The degree of dissolution, as measured through the preservation of *C. leptoporus*, is high in core GC-3 in comparison with cores RC12-113 and Z-2108. The dissolution patterns of three cores do not show a systematic correspondence with the $\delta^{18}O$ record. Of interest, however, are the good preservation peaks that are recognized in all three cores at the transitions from glacial to interglacial events.

(6) The apparent relation between low percentage values for *F. profunda* in core GC-3 located near the STC today, and high dissolution recognized through the *C. leptoporus* index, remains unclear. This tends to suggest that the link between the position of the nutricline in the Turbulent Boundary Layer and wind strengthening, as demonstrated for the tropical Atlantic Ocean by Molfino and McIntyre (1990a,b), is not obvious for such a site located at a high latitude.

(7) A transfer function for estimating past-SST using calcareous nannoplankton still awaits the light of day. Additional modern environmental parameters are necessary to decipher the temperature signal from other variables.

Acknowledgements

The senior author (C.H.) wishes to thank Professor Hisatake Okada, Hokkaido University, for his useful advice and constructive criticisms during this project. He is also very grateful to JAPEX for permission to publish this paper. The stable-isotope measurements for core GC-3 were provided by the Research School of Earth Sciences at ANU.

We also thank the members of the Australian Marine Quaternary Program for their helpful comments and encouragement, and Mr. R. Cunningham for his help with statistical treatment of the data.

References

Anderson, D.M., Prell, W.L., Barratt, N.J., 1989. Estimates of sea surface temperature in the Coral Sea at the last glacial maximum. Paleoceanography 4, 615–627.

Dudley, W.C., Nelson, C.S., 1988. The $\delta^{13}C$ content of calcareous nannofossils as an indicator of Quaternary paleoproductivity in the Southwest Pacific region. N.Z. J. Geol. Geophys. 31, 111–116.

Dudley, W.C., Nelson, C.S., 1989. Quaternary surface-water stable isotope signal from calcareous nannofossils at DSDP Site 593, southern Tasman Sea. Mar. Micropaleontol. 13, 353–373.

Gartner, S., 1977. Calcareous nannofossil biostratigrapy and revised zonation of the Pleistocene. Mar. Micropaleontol. 2, 1–25.

Hiramatsu, C., De Deckker, P., 1996. The distribution of calcareous nannoplankton near the Subtropical Convergence, south of Tasmania, Australia. Mar. Freshwater Res. 47, 707–713.

Hiramatsu, C., De Deckker, P., 1997. Calcareous nannoplankton assemblages of surface sediments in the Coral and Tasman Seas. Palaeogeogr., Palaeoclimatol., Palaeoecol. 131, 257–285.

Honjo, S., 1975. Dissolution of suspended coccoliths in the deep-sea water column and sedimentation of coccolith ooze. Cushman Found. Foraminiferal Res., Spec. Publ. 15, 114–128.

Lohman, W.H., 1986. Calcareous nannoplankton biostratigraphy of the southern Coral Sea, Tasman Sea, and southwestern Pacific Ocean, Deep Sea Drilling Project Leg 90: Neogene and Quaternary. Init. Rep. DSDP 90, 763–793.

Martinez, J.I., 1994. Late Pleistocene palaeoceanography of the Tasman Sea: Implications for the dynamics of the warm pool in the western Pacific. Palaeogeogr., Palaeoclimatol., Palaeoecol. 112, 19–62.

Martinson, D.G., Pisias, N.G., Hays, J.D., Imbrie, J., Moore, T.C., Jr., Shackleton, N.J., 1987. Age dating and the orbital theory of the ice ages: development of a high resolution 0–300,000 year chronostratigraphy. Quat. Res. 27, 1–29.

Matsuoka, H., 1990. A new method to evaluate dissolution of $CaCO_3$ in deep-sea sediments. Trans. Proc. Paleontol. Soc. Jpn. 157, 430–434.

Matsuoka, H., Okada, H., 1989. Quantitative analysis of Quaternary nannoplankton in the subtropical Northwestern Pacific Ocean. Mar. Micropaleontol. 14, 97–118.

Molfino, B., McIntyre, A., 1990a. Precessional forcing of nutricline dynamics in the equatorial Atlantic. Science 249, 766–769.

Molfino, B., McIntyre, A., 1990b. Nutricline variation in the equatorial Atlantic coincident with the Younger Dryas. Paleoceanography 5, 997–1008.

Nelson, C.S., Hendy, C.H., Dudley, W.C., 1985. Quaternary isotope stratigraphy of Hole 593, Challenger Plateau, south Tasman Sea; preliminary observations based on foraminifers and calcareous nannofossils. Init. Rep. DSDP 90, 1413–1424.

Nelson, C.S., Hendy, C.H., Cuthbertson, A.M., 1993. Compendium of stable oxygen and carbon isotope data for the Late Quaternary interval of deep-sea cores from the New Zealand sector of the Tasman Sea and Southwest Pacific Ocean. Dep. Earth Sci., Univ. Waikato, Occas. Rep. 16, 1–87.

Okada, H., 1992. Biogeographic control of modern nannofossil assemblages in surface sediments of Ise Bay, Mikawa Bay and Kumano-nada, off coast of central Japan. Mem. Sci. Geol., Mem. Ist. Geol. Mineral., Univ. Padova 43, 431–449.

Okada, H., Honjo, S., 1973. The distribution of oceanic coccolithophorids in the Pacific. Deep-Sea Res. 20, 355–374.

Okada, H., McIntyre, A., 1977. Modern coccolithophores of the Pacific and North Atlantic Oceans. Micropaleontology 23 (1), 1–55.

Okada, H., Wells, P., 1994. Late Quaternary nannofossil indicators of climatic change in deep-sea cores RC9-150 and RS96GC21 off Western Australia. In: The Late Quaternary History of Oceans in the Australasian Region: Comparison with the Atlantic Record. Geol. Dep., Aust. Natl. Univ., Canberra, A.C.T., Nov. 1994 (abstract).

Roth, P.H., Berger, W.H., 1975. Distribution and dissolution of coccoliths in the north and central Pacific. Cushman Found. Foraminiferal Res., Spec. Publ. 13, 87–113.

Takayama, T., Sato, T., 1987. Coccolith biostratigraphy of the North Atlantic Ocean, Deep Sea Drilling Project Leg 94. Init. Rep. DSDP 94, 651–702.

Thiede, J., 1979. Wind regimes over the late Quaternary southwest Pacific Ocean. Geology 7, 259–262.

Thierstein, H.R., Geitzenauer, K.R., Molfino, B., Shackleton, N.J., 1977. Global synchroneity of late Quaternary coccolith datum levels: validation by oxygen isotopes. Geology 5, 400–404.

Yanagisawa, Y., 1993. Note on diatom temperature index (T_d). Fossils 55, 1–8 (in Japanese, with English abstract).

Young, J.R., Westbroek, P., 1991. Genotypic variation in the coccolithophorid species *Emiliania huxleyi*. Mar. Micropaleontol. 18, 5–23.